VI International Conference on Particle-based Methods – Fundamentals and Applications
PARTICLES 2019
E. Oñate, M. Bischoff, D.R.J. Owen P. Wriggers, , & T. Zohdi (Eds)

# FLID-SOLID MULTIPHASE FLOW SIMULATOR USING A SPH-DEM COUPLED METHOD IN CONSIDERATION OF LIQUID BRIDGE FORCE RELATED TO WATER CONTENT

**KUMPEI TSUJI [1] AND MITSUTERU ASAI [2]**

[1] Department of Civil Engineering, Graduate School of Engineering, Kyushu University
Motoka744, Nishi-ku, Fukuoka 819-0395, JAPAN
e-mail: tsuji@doc.kyushu-u.ac.jp,
web page: https://kyushu-u.wixsite.com/structural-analysis

[2] Ph.D., Associate Prof., Department of Civil Engineering, Graduate School of Engineering, Kyushu University
Motoka744, Nishi-ku, Fukuoka 819-0395, JAPAN
e-mail: asai@doc.kyushu-u.ac.jp,
web page: https://kyushu-u.wixsite.com/structural-analysis

**Key words:** Fluid-Solid multiphase flow, SPH, DEM, Liquid bridge force, Ground collapse.

**Abstract.** Most of the recent natural disasters such as landslide and tsunamis are complex phenomena in which fluid, ground, structures, etc. affect each other. Therefore, it is necessary to study from various mechanical viewpoints. Among them, in this research, we focus on "soil-water mixed phase flow" where fluid and soil affect each other, such as slope failure and ground collapse. In this study, ISPH method is applied for fluid simulation while DEM is applied for modelling of soil behavior. Then, a general-purpose fluid-solid multiphase flow simulator is developed using the ISPH-DEM coupling method. In addition, in DEM analysis, there are problems in consideration of apparent cohesion related to water content. In our analysis method, in order to adapt to unsaturated ground, the liquid bridge force model proposed in the powder technology field.

## 1 INTRODUCTION

In Japan, there are huge inundation damage such as the tsunami disaster caused by the Great East Japan Earthquake and torrential rain disasters that occur frequently in various parts of Japan. In order to prevent such inundation damage, structures such as breakwaters and levees that are generally made of soil should prevent inundation. In the case of disasters occurred in recent years, damage could not be completely prevented and minimized. Now that the frequency of heavy rains is high due to the effects of global warming, and there are concerns about huge earthquakes and tsunamis, numerical analysis techniques are needed to know the limit state of structures such as breakwaters and levees. With these background, our research group has developed multi-scale and multi-physics disaster simulator based on particle method in order to estimate the level of damage caused by unexpected natural disasters. Among them, we are developing a fluid-soil multiphase flow simulator for seepage failure, scour failure and ground collapse phenomenon. In this simulator, SPH (Smoothed Particle Hydrodynamics) is applied for fluid simulation, and DEM (Discrete Element Method) is applied for soil behavior

analysis. And coupled analysis is performed through the empirical interaction force of both. In the previous study [1], the seepage and scouring analysis of the breakwater mound is analyzed, and its validity has been confirmed from the comparison with the experiment. In this research, the effect of apparent cohesion with moisture is newly introduced to expand the target area to unsaturated ground. Using the above analysis method, it is reproduced the ground collapse phenomenon that is with few examples. The ground collapse phenomenon is a large deformation and discrete phenomenon accompanied by the segregation of soil masses, and this method based on the particle method is one of the suitable examples.

## 2 SPH-DEM COUPLED ANALYSIS MODEL

A coupled model of SPH and DEM is important in the multiphase flow analysis. There are two models to couple those methods, one is the "Direct pressure model" we call. In general, a solid in fluid is moved by receiving a dynamic pressure from fluid. In this direct pressure model, a solid also moves in same way. However, if this model is adopted, the diameter of fluid particles need to be much smaller than the solid to calculate a force acting on its surface accurately. It is not desirable to adopt such a computationally expensive method to carry out the real-scale analysis that we aiming for. The other method is "Interaction force model". In this methods, a fluid particle can overlap with solid particles, and a fluid pressure don't act on its surface. Instead of a pressure, an interaction force acts on each particle, a resistance force on fluid and a drag force on solid. In addition, the diameter of fluid particle can be almost the same size with a solid particle. Then, the latter coupled model is adopted because it is possible to reduce the computational cost by using "Interaction force model".

## 3 ANALYSIS METHOD OF EACH PHASE

### 3.1 The unified governing equation

In fluid-solid(soil) multiphase flow analysis, fluid flow is regarded as free surface flow in the fluid region and seepage flow in the ground. According to Akbari, H. [2], a unified governing equation modeled to solve free surface flow and seepage flow continuously can be written as:

$$\frac{C_r(\varepsilon)}{\varepsilon}\frac{D\overline{\boldsymbol{v}}_f}{Dt} = -\frac{1}{\rho_f}\nabla P + \boldsymbol{g} + \nu_E(\varepsilon)\nabla^2\overline{\boldsymbol{v}}_f - a(\varepsilon)\overline{\boldsymbol{v}}_f - b(\varepsilon)\overline{\boldsymbol{v}}_f\left|\overline{\boldsymbol{v}}_f\right| \tag{1}$$

$$\frac{D\bar{\rho}_f}{Dt} + \bar{\rho}_f\nabla\cdot\left(\frac{\overline{\boldsymbol{v}}_f}{\varepsilon}\right) = 0 \tag{2}$$

where $\rho_f$, $\boldsymbol{g}$, $P$ and $\varepsilon$ represent the original fluid density, the gravitational acceleration, the fluid pressure and the porosity. $\overline{\boldsymbol{v}}_f$ is the Darcy velocity which is understood as a spatially averaged velocity given by $\overline{\boldsymbol{v}}_f = \varepsilon\boldsymbol{v}_f$, $\boldsymbol{v}_f$ is the intrinsic fluid velocity. Here, $\bar{\rho}_f$ denotes the apparent density, which is given by $\bar{\rho}_f = \varepsilon\rho_f$. This relation regarding the apparent density is necessary to be employed in order to satisfy the volume conservation of fluid inside the porous medium. Some of the coefficient are defined as:

$$C_r(\varepsilon) = 1 + 0.34\frac{1-\varepsilon}{\varepsilon} \tag{3}$$

$$\nu_E(\varepsilon) = \frac{\nu_w + \nu_T}{\varepsilon} \tag{4}$$

$$a(\varepsilon) = \alpha_c \frac{\nu_w(1-\varepsilon)^2}{\varepsilon^3 {d_s}^2} \tag{5}$$

$$b(\varepsilon) = \beta_c \frac{(1-\varepsilon)}{\varepsilon^3 d_s} \tag{6}$$

where $C_r(\varepsilon)$ is the inertial coefficient to evaluate the additional resistance force caused by the virtual mass, while $\nu_E(\varepsilon)$ is the effective viscosity including the kinematic viscosity of the fluid $\nu_w$ and the turbulent viscosity $\nu_T$. The Smagorinsky model is adopted to define the eddy viscosity. $a(\varepsilon)$ and $b(\varepsilon)$ are the linear and non-linear coefficients, $\alpha_c$ and $\beta_c$ in these equation are defined as the constant in our analysis. Moreover, $d_s$ is the diameter of a solid particle. Here, the fourth and fifth terms in right side of Eq. (1) means the resistance force from the porous medium. This unified governing equation is proposed by Akbari to represent the seepage flow in a fixed porous medium with a low porosity. However, in the floating soil or on the soil mass surface, the soil as a porosity medium also moves and the porosity comes to be high. Therefore, the resistance force terms in Eq. (1) are modified referring to Wen and Yu [3], and the unified governing equation is rewritten as:

$$\frac{C_r(\varepsilon)}{\varepsilon}\frac{D\overline{\boldsymbol{v}}_f}{Dt} = -\frac{1}{\rho_f}\nabla P + \boldsymbol{g} + \nu_E(\varepsilon)\nabla^2\overline{\boldsymbol{v}}_f \begin{cases} -a(\varepsilon)\varepsilon\boldsymbol{v}_r - b(\varepsilon)\varepsilon^2\boldsymbol{v}_r|\boldsymbol{v}_r| & (\varepsilon < 0.8) \\ -c(\varepsilon)\boldsymbol{v}_r|\boldsymbol{v}_r| & (\varepsilon \geq 0.8) \end{cases} \tag{7}$$

Here, in considering the movement of the porous medium, the velocity in resistance force terms is changed to relative velocity $\boldsymbol{v}_r$ between fluid and solid which is given by $\boldsymbol{v}_r = \boldsymbol{v}_f - \boldsymbol{v}_s$. In taking a relative velocity, the fluid velocity must not be a spatially averaged velocity $\overline{\boldsymbol{v}}_f$ but an original velocity $\boldsymbol{v}_f$. Thus, the porosity $\varepsilon$ is multiplied by the linear and non-linear coefficients. In addition, the resistance force proposed by Wen and Yu for the high porosity domain ($\varepsilon \geq 0.8$) is considered. $C_d$ is drag coefficient and defined with Reynolds number $R_e$ as follows:

$$C_d = \frac{24\{1 + 0.15 * {R_e}^{0.687}\}}{R_e} \quad (R_e \leq 1000) \tag{8}$$

$$C_d = 0.43 \quad (R_e > 1000) \tag{9}$$

$$R_e = \frac{\varepsilon\rho_f d_s|\boldsymbol{v}_f - \boldsymbol{v}_s|}{\mu_f} \tag{10}$$

According to Eq.(7), the fluid flow outside the porous medium can be given by the Navier-Stokes equation with the porosity $\varepsilon = 1$. On the other hand, the fluid flow inside the porous medium can be described by including the resistance force. Eq. (2) represents the unified continuity equation for a compressible fluid.

The resistance force in Eq. (7) acts on fluid as a resistance force, and it needs to act on the porous medium as a drag force in the opposite sign as well to satisfy the action-reaction law. Thus, this resistance force can be considered as the interaction force between fluid and solid.

### 3.2 SPH Formulation

In this paper, the Smoothed Particle Hydrodynamics (SPH) method is adopted to solve the unified governing equation for free surface and seepage flow. The basic concept in SPH method is that for any function $\phi$ attached to particle "$i$" located at $\boldsymbol{x}_i$ is represented by the following volume summation of contributions from neighbor particles:

$$\phi(\boldsymbol{x}_i) \approx \langle \phi_i \rangle := \sum_j \frac{m_j}{\rho_j} \phi_j W(r_{ij}, h) \tag{11}$$

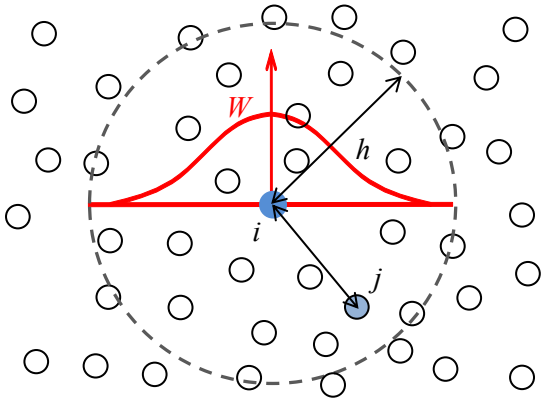


**Figure 1**: Particle placement and influence radius in the SPH

where $m$ and $W$ are the representative volume of particle and a weight function known as the smoothing kernel function. In this paper, the "Cubic B-Spline function" is adopted as the kernel function. $j$ is a particle in the smoothing length $h$ and $r_{ij}$ is the length of the relative coordinate vector $\boldsymbol{r}_{ij}(= \boldsymbol{x}_j - \boldsymbol{x}_i)$. In this study, the smoothing length set to 2.4 times the initial diameter of the particle. Note that, the triangle bracket $\langle \phi_i \rangle$ means SPH approximation of a function $\phi$. The divergence $\nabla \cdot \phi$, the gradient $\nabla \phi$ and the Laplacian $\nabla^2 \phi$ can be assumed by using the above defined SPH approximation as follows:

$$\langle \nabla \cdot \phi_i \rangle = \rho_i \sum_j m_j \left( \frac{\phi_j}{{\rho_j}^2} + \frac{\phi_i}{{\rho_i}^2} \right) \cdot \nabla W(r_{ij}, h) \tag{12}$$

$$\langle \nabla \phi_i \rangle = \rho_i \sum_j m_j \left( \frac{\phi_j}{{\rho_j}^2} + \frac{\phi_i}{{\rho_i}^2} \right) \nabla W(r_{ij}, h) \tag{13}$$

$$\langle \nabla^2 \phi_i \rangle = \sum_j m_j \left( \frac{\rho_i + \rho_j}{\rho_i \rho_j} \frac{\boldsymbol{r}_{ij} \cdot \nabla W(r_{ij}, h)}{{\boldsymbol{r}_{ij}}^2 + \eta^2} \right) (\phi_i - \phi_j) \tag{14}$$

$\eta$ is the parameter to avoid division by zero and defined by the following expression $\eta^2 = 0.0001(h/2)^2$.

### 3.3 Formulation of the unified governing equation in the stabilized ISPH method

In this paper, fluid analysis is performed using the stabilized Incompressible SPH method proposed by Asai et al. [4]. In the ISPH method, the governing equations of incompressible fluid are time discretized by a separate method called a projection method based on the predictor modifier method, and the separated equations are spatially discretized based on the basic

formula of SPH method. In this method, the pressure is calculated implicitly and the velocity fields are updated explicitly. In this study, the same idea of ISPH for the Navier-Stoke equation is applied to solve the unified governing equation, Eq. (2) and Eq. (7). To begin with the discretization, $\overline{\boldsymbol{v}}_f$ at $n+1$ step is written as:

$$\overline{\boldsymbol{v}}_f^{n+1} = \overline{\boldsymbol{v}}_f^* + \Delta\overline{\boldsymbol{v}}_f^* \tag{15}$$

where $\overline{\boldsymbol{v}}_f^*$ and $\Delta\overline{\boldsymbol{v}}_f^*$ are the predictor term and the corrector term. Based on the projection method. Eq. (7) can be separated as:

$$\overline{\boldsymbol{v}}_f^* = \overline{\boldsymbol{v}}_f^n + \frac{\varepsilon\Delta t}{C_r(\varepsilon)}\left(\boldsymbol{g} + \nu_E(\varepsilon)\nabla^2\overline{\boldsymbol{v}}_f^n - \boldsymbol{\gamma}^n\right) \tag{16}$$

$$\Delta\overline{\boldsymbol{v}}_f^* = \frac{\varepsilon\Delta t}{C_r(\varepsilon)}\left(-\frac{1}{\rho_f}\nabla P^{n+1}\right) \tag{17}$$

where $\boldsymbol{\gamma}$ summatizes the resistance terms in Eq. (7) at $n$ step. The pressure $P^{n+1}$ in Eq. (19) is determined by the Pressure Poisson Equation as follows:

$$\nabla^2 P^{n+1} = \frac{C_r(\varepsilon)\rho_f}{\varepsilon\Delta t}\nabla\cdot\overline{\boldsymbol{v}}_f^* \tag{18}$$

During numerical simulation, the 'particle' density may change slightly from the initial value because the particle density is strongly dependent on particle locations in the SPH method. If the particle distribution can keep almost uniformity, the difference between 'physical' and 'particle' density may be vanishingly small. In other words, accurate SPH results in incompressible flow need to keep the uniform particle distribution. For this purpose, the different source term in the pressure Poisson equation can be derived using the 'particle' density. In stabilized ISPH method, the pressure Poisson equation (18) reformulated as:

$$\langle\nabla^2 P^{n+1}\rangle \approx \frac{C_r(\varepsilon)}{\varepsilon}\left(\frac{\rho_f}{\Delta t}\langle\nabla\cdot\overline{\boldsymbol{v}}_f^*\rangle + \alpha\frac{\bar{\rho}_f^n - \langle\bar{\rho}_f^n\rangle}{\Delta t^2}\right) \tag{19}$$

where $\alpha$ is called as the relaxation coefficient and is generally set to be much less than 1.0. In this study, $\alpha$ is set to 0.01. The analysis with the stabilized ISPH method can get good conservation of volume.

### 3.4 The equation of motion of soil

In this study, the behavior of the soil particles constituting the ground is analyzed by Discrete Element Method (DEM). Here, the soil particles were modeled as spherical DEM particles, its diameter is $d_s$. In general, the contact detection is done every time step and a DEM particle moves by receiving the contact forces in DEM. In addition to that, the fluid force also acts on the DEM particles in the fluid domain. There some kinds of the fluid forces, however the all of them don't influence the particle motion. In this study, the buoyancy force and drag force are adopted to the fluid forces, the equation of motion of soil in fluid is written as follows with the contact force:

$$m_s\frac{d\boldsymbol{v}_s}{dt} = m_s\boldsymbol{g} - \nabla PV_s + \boldsymbol{F}_d + \sum\boldsymbol{F}_c + \sum\boldsymbol{F}_{coh} \tag{20}$$

$$\boldsymbol{F}_d = \begin{cases} (a(\varepsilon)\varepsilon^2\boldsymbol{v}_r + b(\varepsilon)\varepsilon^3\boldsymbol{v}_r|\boldsymbol{v}_r|)\dfrac{V_s}{1-\varepsilon} & (\varepsilon < 0.8) \\ (-c(\varepsilon)\boldsymbol{v}_r|\boldsymbol{v}_r|)\dfrac{V_s}{1-\varepsilon} & (\varepsilon \geq 0.8) \end{cases} \tag{21}$$

where $m_s$, $\boldsymbol{v}_s$ and $V_s$ are the mass, the velocity and the volume of a soil particle respectively. The second and third terms in right side are the fluid forces, the second is the buoyancy force and the third $\boldsymbol{F}_d$ is the drag force. $\boldsymbol{F}_c$ means the contact force between DEM particles. $\boldsymbol{F}_{coh}$ means the apparent cohesive force related to water content, which is explained in a 3.6 section. The drag force $\boldsymbol{F}_d$ has the same meaning as the interaction force. Therefore, the resistance force for fluid is adopted to the drag force for soil. The drag force acting on one particle is given by Eq. (21).

The equation of angular motion for the spherical DEM is written as:

$$I\frac{d\boldsymbol{\omega}}{dt} = \sum \boldsymbol{T} \tag{22}$$

The contact force between the particles or particle-wall is calculated by the intrusion of a particle with a spring-dashpot model in DEM. The contact force $\boldsymbol{F}_c$ is divided into two components, a repulsive force in the normal direction $\boldsymbol{F}_c^n$ and a friction force in the tangential direction $\boldsymbol{F}_c^t$, and described as:

$$\boldsymbol{F}_c = \boldsymbol{F}_c^n + \boldsymbol{F}_c^t \tag{23}$$

$$\boldsymbol{F}_c^n = (-k\delta^n - \eta|\boldsymbol{v}_r^n|)\boldsymbol{n} \tag{24}$$

$$\boldsymbol{F}_c^t = \begin{cases} (-k\delta^n - \eta|\boldsymbol{v}_r^t|)\boldsymbol{t} & |\boldsymbol{F}_c^t| < \mu|\boldsymbol{F}_c^n| \\ -\mu|\boldsymbol{F}_c^n|\boldsymbol{t} & |\boldsymbol{F}_c^t| \geq \mu|\boldsymbol{F}_c^n| \end{cases} \tag{25}$$

$$\eta = -2ln\,(e)\sqrt{\frac{k}{ln^2(e)+\pi^2}\frac{2m_i m_j}{m_i+m_j}} \tag{26}$$

where $k$, $\delta$, $\eta$, $\boldsymbol{n}$ , $\boldsymbol{t}$ and $e$ are the stiffness, the displacement, the damping coefficient, normal, tangential unit vector and the coefficient of restitution.

The equation of angular motion for the spherical DEM is written as follows. The torque is calculated from the tangential contact force.

$$I\frac{d\boldsymbol{\omega}}{dt} = \sum \boldsymbol{T} = \sum \boldsymbol{l} \times \boldsymbol{F}_c^t \tag{27}$$

where $\boldsymbol{l}$ indicates the vector from the center of a particle to a contact point.

### 3.5 Rolling friction

In order to reduce the calculation cost, DEM analysis is carried out using spherical particles whose contact judgment is relatively easy. However, real soil particles have unique concave and convex shapes, and it is impossible to express steep deposition shape. Therefore, in this research, rolling friction is introduced, which is an additional force artificially suppressing particle rotation. There are many rolling friction models proposed from the past research. Among them, in this study, rolling friction proposed by Fukumoto et al.[5] is used, and described as follows:

$$\boldsymbol{M_r} = |\boldsymbol{F}_n|a\hat{\boldsymbol{\omega}} = |\boldsymbol{F}_n|\lambda r'\hat{\boldsymbol{\omega}} = \lambda\sqrt{L(2r-L)}|\boldsymbol{F_n}|\hat{\boldsymbol{\omega}} \tag{28}$$

where $r$, $\boldsymbol{F}_n$, $\hat{\boldsymbol{\omega}}$ and $L$ are the radius of particle, the acting force in the normal direction, unit angular velocity vector and displacement. $b$ is the rolling friction coefficient representing the shape characteristic. And also, using a soil sample to be analyzed, examination was conducted by simple preliminary analysis as shown in the next chapter.

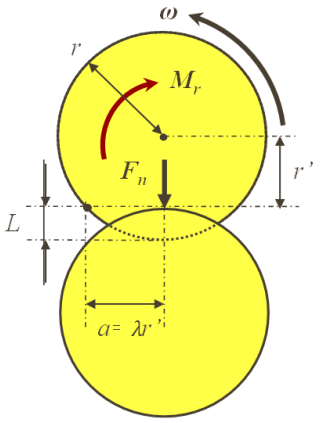


**Figure 2**: Rolling friction model

### 3.6 Apparent cohesive force

The method up to the previous section did not take into consideration of the cohesion effect related to the water content of the soil in the unsaturated ground. Depending on its moisture content, the soil forms aggregate shapes by sticking particles together, and the soil clumps become self-supporting. Therefore, by incorporating the effect of the apparent cohesive force into the method, a DEM analysis adapted to dry, saturated and unsaturated state is developed. In this study, the liquid bridge force model proposed by X. Sun et al. [6] is adopted as the apparent cohesive force related to the water content of the soil particles. This force model is presented based on a toroidal approximation of the liquid bridge profile. Its advantage resides in generality, which is applicable to a wide range of liquid volumes, contact angles and radius ratios. In addition, Laplace pressure, which is a suction in soil mechanics, can be taken into consideration. However, since spherical DEM particles are used in this study, the presence of fine particles filling the gaps is ignored. Then, the apparent cohesion, in particular Laplace pressure, is underestimated. In addition, suction is a field that has been studied in soil mechanics, so there is no mechanical model that can be used for DEM. In order to take account of this effect, a conversion parameter $\kappa$ is introduced to the model proposed by X.Sun et al. , and this value is adjusted by comparison with a simple experiment.

$$\boldsymbol{F}_{coh} = \kappa(\Delta p \pi {\rho_{in}}^2 + 2\pi\gamma\rho_{in})\boldsymbol{n} \tag{29}$$

where $\Delta p$, $\rho_{in}$, $\gamma$ and $\boldsymbol{n}$ are the Laplace pressure, the internal radius of the liquid bridge, surface tension and unit normal vector.

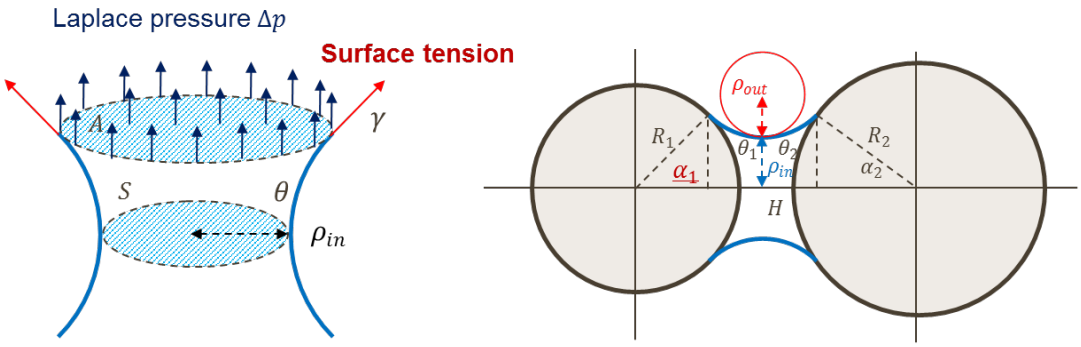


**Figure 3**: Liquid force model [6]

## 4 DETERMINATION OF VARIOUS PARAMETERS

It is necessary to identify various parameters corresponding to material property values in advance. Firstly, a pulling test of a cylindrical specimen filled with soil sample is carried out, and various parameters are identified. A simple experiment with dry soil are carried out to identify the rolling friction coefficient $\lambda$. Next, a series of experimental test with different water contents is carried out to identify the apparent parameter $\kappa$ for estimating the magnitude in the apparent cohesion force.

### 4.1 Rolling friction parameter $\lambda$

Using the soil sample used in the road caving collapse experiment, a cylindrical specimen pulling test with a diameter of 5 cm and a height of 10 cm was repeated ten times, and an angle of repose of 26.5 degrees was obtained. As a result of the reproduction DEM analysis, when $\lambda = 0.9$, the angle closest to the repose angle of the experiment, and the same diameter as the sand cone after the experiment was obtained. Therefore, $\lambda = 0.9$ is adopted in this research.

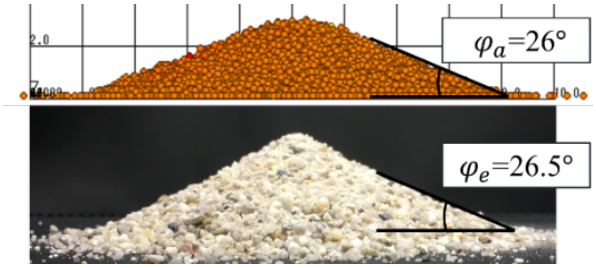


**Figure 4**: Comparison of angle of repose in experiment and DEM analysis

### 4.2 Conversion parameter $\kappa$ in apparent cohesive force

Next, in order to reproduce the collapse behavior of unsaturated soil, the same experiment as previous one using wet sand. In the tests where water content was different, we focused on

the results of rapid lateral deformation after temporary stabilization. This time, the magnitude of the conversion parameter ($\kappa = 15$) required to reproduce this result was determined by DEM analysis.

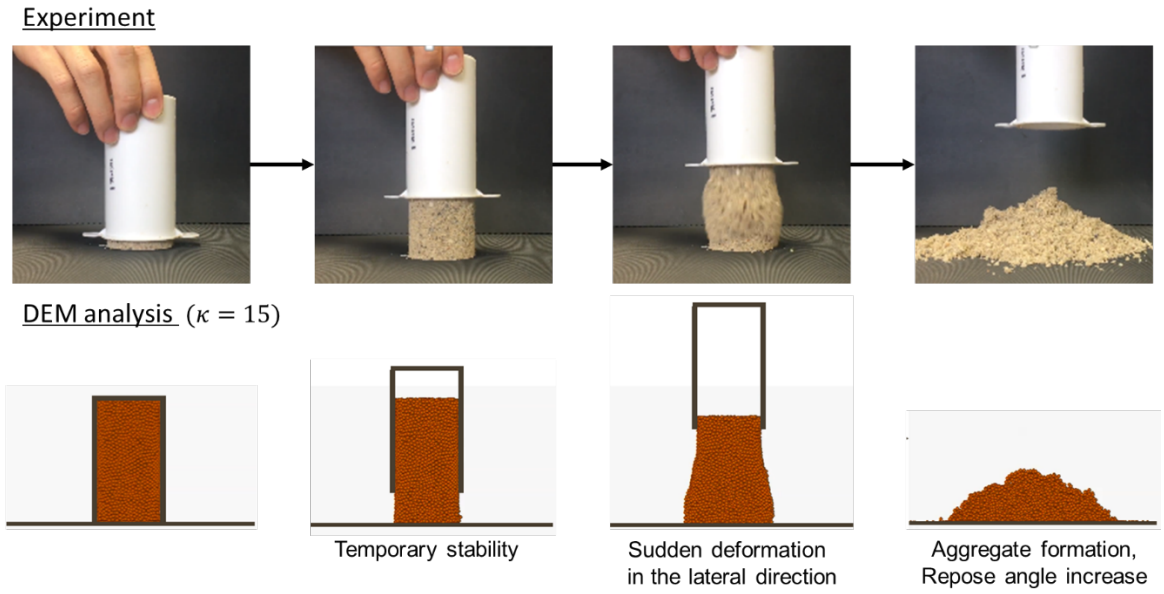


**Figure 5**: Comparison of angle of repose in experiment and DEM analysis

## 5 ANALYSIS OF GROUND COLLAPSE PHENOMENON

In this research, we focused on the qualitative reproduction of the ground collapse process in the reproduction experiment of the ground collapse phenomenon under the condition corresponding to the experiment conducted by Konishi et al.[7]. A small ground model with a width of 300 mm, a height of 200 mm and a depth of 50 mm is prepared as an analysis model shown as follows.

**Table 1:** Analysis condition

| **Water (SPH)** | | |
|---|---|---|
| Numbers of particles | Particle size [cm] | Density [g/cm$^3$] |
| 12,626 | 0.3 | 1 |
| **Soil (DEM)** | | |
| Numbers of particles | Particle size [cm] | Density [g/cm$^3$] |
| 132,124 | 0.3 | 2.6 |
| Restitution coefficient | Spring constant[N/m] | Friction coefficient |
| 0.5 | 1000 | 0.57 |
| Rolling friction coefficient λ | | Conversion parameter α |
| 0.9 | | 15 |

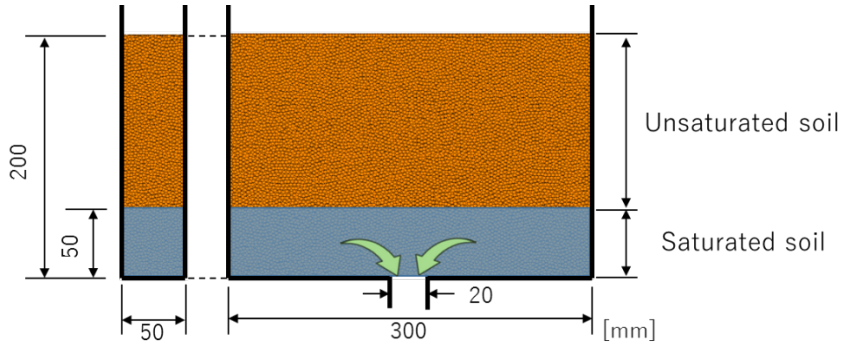


**Figure 6**: The small model of ground collapse phenomenon

### 5.1 Analysis without water level (only DEM analysis)

At first, the movement of soil particles of wet and dry sand is compared by the presence of apparent cohesion without considering groundwater level. In the case of dry sand analysis, cohesion is not considered, and in the case of wet sand analysis, it is considered.

As a result of the analysis of dry sand, the velocity distribution spreads to the left and right with time, and it has been confirmed that it flows out without stopping like an hourglass. On the other hand, in the case of wet sand, the outflow velocity of soil particles decreased significantly. Furthermore, since the velocity distribution is concentrated around the outflow hole, it can be said that the localization of the behavior can also be reproduced. In the analysis where the cohesion is increased, it is confirmed that the self-supporting of soil mass and the outflow of soil particles stopped. From the above results, it is considered that the behavior of wet sand can be reproduced and verified qualitatively by introducing the effect of adhesion. However, when there is no water, it is not possible to reproduce the hollows and occurring the ground collapse phenomenon.

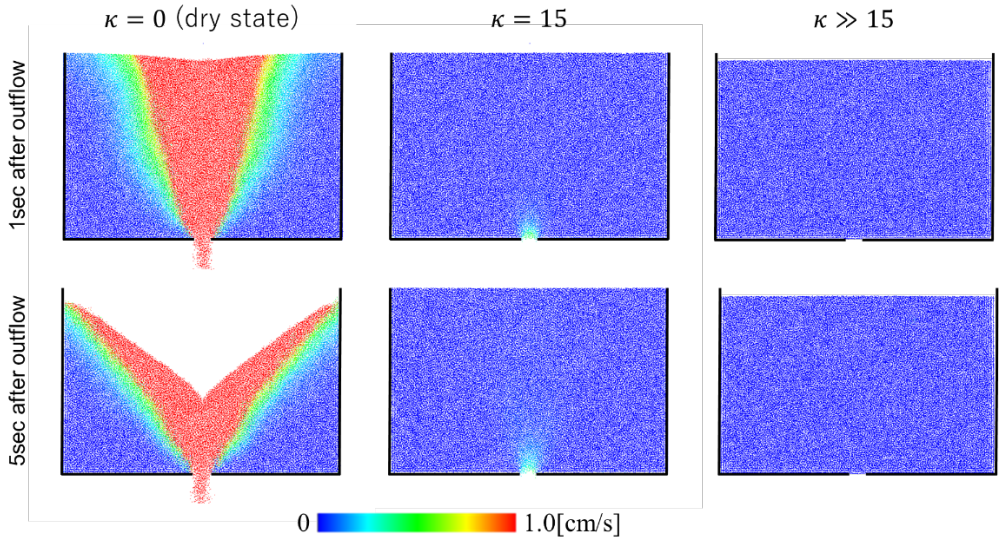


**Figure 7**: Analysis result without groundwater level (downward velocity ditribution)

### 5.2 Analysis with water level (SPH-DEM coupled analysis)

Next, a water level of 5 cm in height was set as groundwater, and coupled analysis of water (SPH) and soil (DEM) is carried out. In this case, both unsaturated and saturated ground give apparent cohesive force in DEM calculation. The saturated ground below the groundwater level was set to be smaller than the cohesive force of the unsaturated ground.

As a result, due to a large difference in apparent cohesive force near the free surface and the outflow of water, a hollow grows in the horizontal direction, and the ceiling is destabilized, collapsing, collapsing soil drainage, and repeating arched stability of the ceiling…The situation was confirmed.

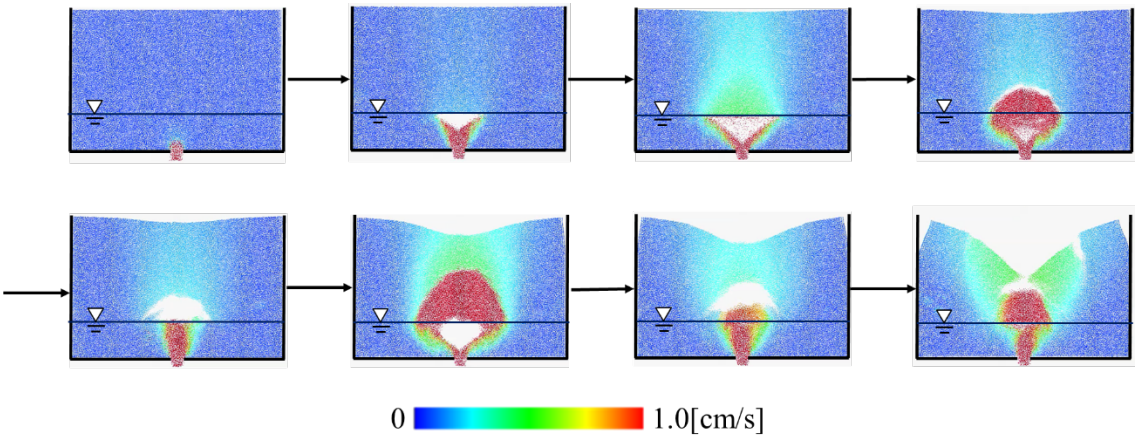


**Figure 8**: Analysis result with groundwater level (downward velocity ditribution)

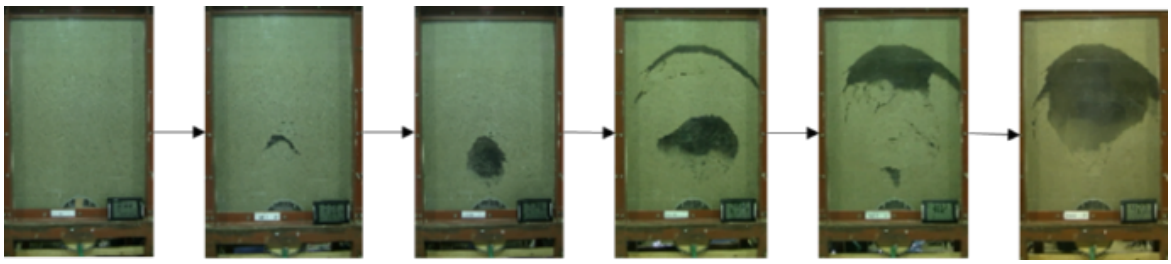

**Figure 9**: Experiment result conducted by Konishi et al.[7]

The same tendency of collapse has been confirmed in the experiment of Konishi et al. From this study, by carrying out coupled analysis of SPH and DEM, it was possible to show the collapse behavior of the ground sink which has not been reproduced so far.

## 6 CONCLUSIONS

In this study, we tried to analyze the behavior of unsaturated soil considering the apparent cohesion with moisture in the coupled analysis method of the previous research. As a result, in the reproduction analysis of the ground sinking phenomenon, the collapse tendency confirmed in the experiment could be qualitatively reproduced.

Through this research, it was confirmed that the ground collapse phenomenon cannot be reproduced only by increasing the cohesive force. In the future, in addition to the quantitative evaluation of cohesion, we will introduce a cluster DEM model that is composed of can explicitly give the effect of the shape of soil particles without rolling friction. By doing so, sedimentation of the upper ground can be suppressed, and more brittle collapse should be able to be reproduced.

## REFERENCES

[1] K. Harasaki and M. Asai, Validation of a fluid-solid multiphase flow simulation by a SPH-DEM coupled method and soil foundation scour simulation with a coarse graining particle model, Transactions of JSCES, No.20182001, Japan, 2018.

[2] Akbari, H., Modified moving particle method for modeling wave interaction with multi layered porous structures, Coast. Eng., Vol.89, pp.1-19, 2014.

[3] C. Wen. and Y. Yu., Mechanics of fluidization, *Chemical Engineering Progress Symposium Series 62*, 100, 1966.

[4] M. Asai, Aly, AM., Y. Sonoda and Y. Sakai, A stabilized incompressible SPH method by relaxing the density invariance condition, Int. J. for Applied Mathematics, Vol. 2012, Article ID 139583, 2012.

[5] Y. Fukumoto, H.Sakaguchi and A. Murakami, Failure Criteria for Geomaterials in Simple Discrete Element Modeling, Int. J. for Applied Mathematics, Vol.67, No.1, Japan, 2011.

[6] X. Sun, M. Sakai, A liquid bridge model for spherical particles applicable to asymmetric configurations, Chemical Engineering Science, 182: 28-43, 2018.

[7] Y. Konishi, K. Fukunaga, S. Oomine, W. Hukutani and D. Takeuchi, Experimental Study on Risks for Underground Hollows Occurrence and Ground Surface Collapse Due to Underground Sewers, Journal of Japan Sewage Works Association, Vol.5, No.2, Japan (1988).